



Short communication

Ordered mesoporous MoO₂ as a high-performance anode material for aqueous supercapacitorsXinyong Li¹, Jie Shao¹, Jing Li, Li Zhang, Qunting Qu*, Honghe Zheng*

School of Energy & College of Chemistry, Chemical Engineering and Material Science, Soochow University, Suzhou, Jiangsu 215006, China

HIGHLIGHTS

- Ordered mesoporous MoO₂ was prepared using silica KIT-6 as hard template.
- MoO₂ exhibits excellent performance as anode material for aqueous supercapacitors.
- The dominating working ions of MoO₂ in LiOH electrolyte are proved to be Li⁺ ions.

ARTICLE INFO

Article history:

Received 13 February 2013

Received in revised form

25 February 2013

Accepted 2 March 2013

Available online 14 March 2013

Keywords:

Aqueous supercapacitors

Anode

Molybdenum dioxide

Mesoporous

ABSTRACT

Ordered mesoporous MoO₂ is prepared employing silica KIT-6 as hard template. Electrochemical quartz crystal microbalance is utilized to investigate the charge storage mechanism of mesoporous MoO₂ in aqueous LiOH electrolyte solution. The dominating working ions are proved to be Li⁺ ions. Mesoporous MoO₂ exhibits excellent supercapacitive behavior in the potential range of −1.2 to −0.5 V vs. SCE, rendering it a promising anode material for aqueous supercapacitors.

© 2013 Elsevier B.V. All rights reserved.

1. Introduction

Supercapacitors have attracted significant attention owing to their fast charging/discharging ability, ultrahigh power delivery, excellent cycle life, and reliable safety [1,2]. Nonetheless, their energy density is unsatisfactory compared with conventional batteries. According to the formula $E = CU^2/2$, the energy density (E) of a supercapacitor is proportional to its specific capacitance (C) and the square of its operating voltage (U). Numerous researchers have been concentrating on improving the capacitance of various electrode materials through morphology controlling or fabrication of nanocomposites [3,4]. Widening the operating voltage of a supercapacitor, which depends on the potential difference of cathode and anode, is another effective route to enhance energy density. In view of aqueous supercapacitors, lots of cathode materials with working potentials higher than 0 V vs. SCE have been investigated

extensively [5–8], whereas, there are few reports on low-potential (lower than 0 V vs. SCE) anode materials [9–11].

Molybdenum oxides, mainly including MoO₃ and MoO₂, are potential electrode materials for lithium ion batteries [12,13] and supercapacitors [14–18] due to their multiple valence states, high electrochemical activity, and affordable cost. Especially, MoO₂ possesses a strong metallic Mo–Mo bond, rendering it a metal-like conductivity at room temperature [19,20]. Thus MoO₂ is more appealing than other non-conductive transition-metal oxides for supercapacitors application. To the best of our knowledge, MoO₂ has never been reported as an anode material for aqueous supercapacitors. In this work, ordered mesoporous MoO₂ (m -MoO₂) was prepared using (NH₄)₆Mo₇O₂₄·4H₂O as molybdenum source and silica KIT-6 as hard template. m -MoO₂ was demonstrated to exhibit excellent supercapacitive performance benefiting from the ordered mesoporous structure and low solubility of MoO₂ in alkaline LiOH aqueous electrolyte. The average working potential of −0.85 V vs. SCE makes it suitable as an anode material for aqueous supercapacitors. In addition, electrochemical quartz crystal microbalance (EQCM) results prove that the dominating working ions for the charge storage of m -MoO₂ are Li⁺ ions.

* Corresponding authors.

E-mail addresses: qtqu@suda.edu.cn (Q. Qu), hhzheng@suda.edu.cn (H. Zheng).¹ These authors contribute equally to this work.

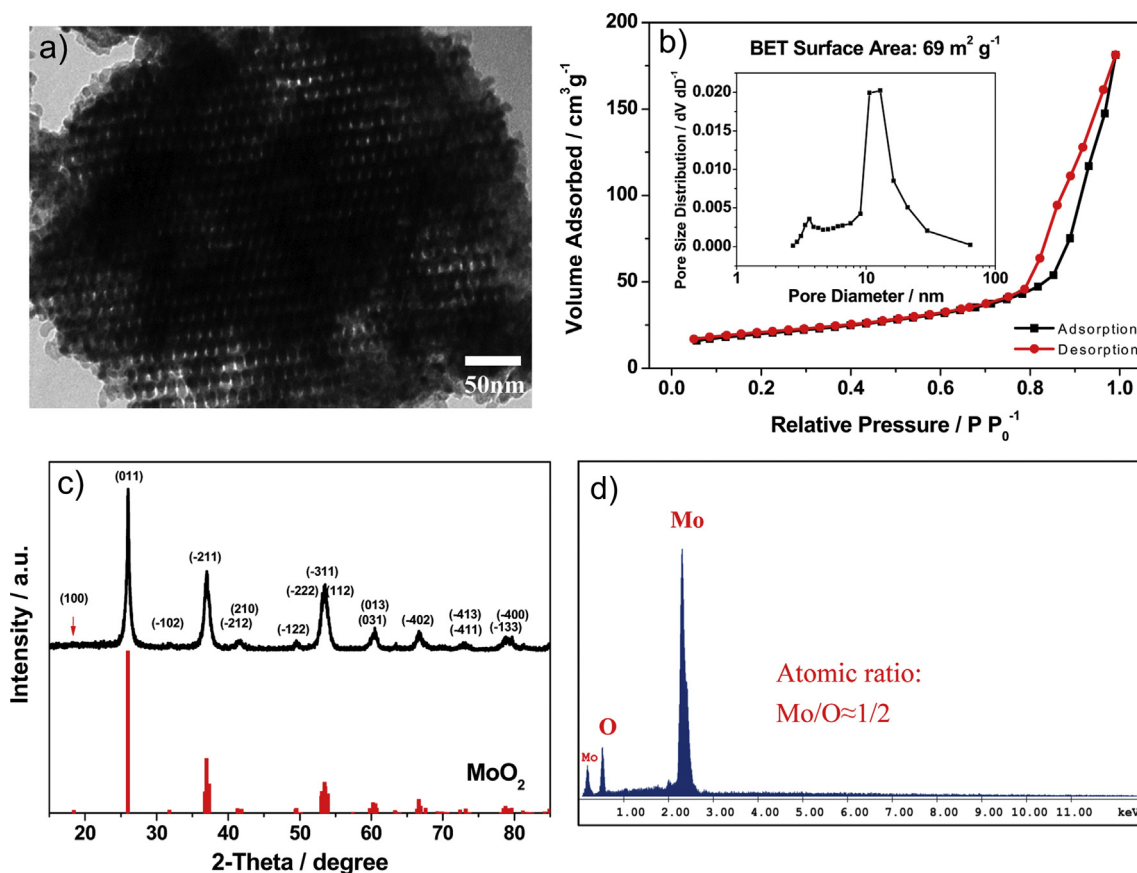


Fig. 1. a) TEM image, b) N_2 sorption isotherms and pore size distribution, c) XRD pattern, and d) EDX spectrum of ordered mesoporous MoO_2 .

2. Experimental

Mesoporous silica KIT-6 was prepared according to the method reported in literature [21]. For the preparation of ordered mesoporous MoO_2 , 1.5 g of $(NH_4)_6Mo_7O_{24} \cdot 4H_2O$ precursor dissolved in 10 mL of deionized water was mixed with 1.0 g of KIT-6 template under stirring in an open crucible. After evaporation of deionized water, the obtained white powders were calcined at 650 °C for 6 h under 5% H_2/Ar atmosphere, which was then etched with 2 M NaOH solution to remove silica template. Bulk MoO_2 was prepared from the direct decomposition of $(NH_4)_6Mo_7O_{24} \cdot 4H_2O$.

Morphologies of the products were observed by scanning electron microscope (SEM, Philips XL30) and transmission electron microscope (TEM, JEOL JEM-2010). The specific surface area and pore size distribution of $m-MoO_2$ were measured according to the Brunauer–Emmett–Teller (BET) method using Micromeritics Tristar II apparatus with liquid nitrogen cooling. X-ray diffraction (XRD) was operated using a Rigaku D/MAX-IIA X-ray diffractometer with Cu $K\alpha$ radiation. Energy dispersive X-ray (EDX) spectrum of $m-MoO_2$ was obtained using Philip XL30 scanning electron microscope. Electrochemical quartz crystal microbalance experiments were carried out on CHI400B EQCM with gold coated quartz crystal electrode. Small amounts of $m-MoO_2$ powder were loaded onto the gold electrode directly for EQCM measurement without addition of any other conductive agents.

Electrochemical performance testing of MoO_2 electrode was operated using a three-electrode cell, in which Ni-mesh and saturated calomel electrode were used as the counter and reference electrode, respectively. The preparation method of MoO_2 working electrode is shown in Supporting information. 1 M LiOH aqueous

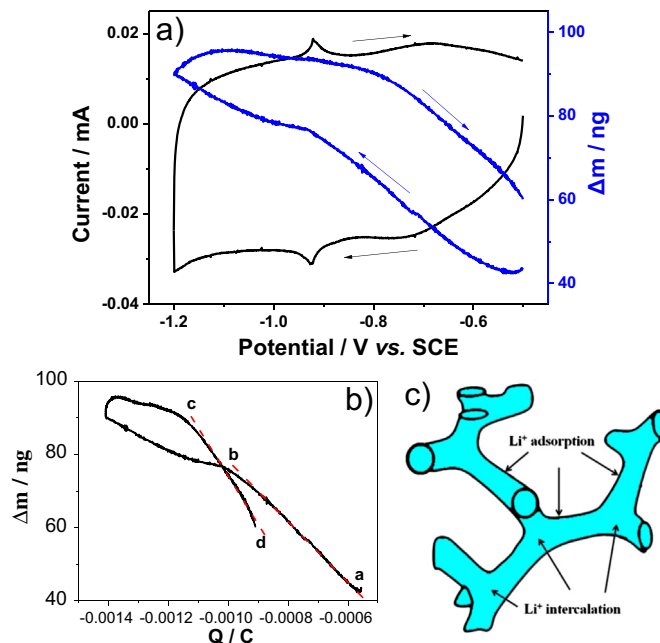


Fig. 2. a) CV curve and mass changes of $m-MoO_2$ electrode obtained through EQCM. The scan rate is set at 15 mV s^{-1} . b) Relation between the mass changes and stored charge of $m-MoO_2$ electrode. The red dash lines are the linear fit of part a–b and c–d. c) Schematic illustration of the charge storage of $m-MoO_2$ including intercalation and adsorption of Li^+ . (For interpretation of the references to colour in this figure legend, the reader is referred to the web version of this article.)

solution was used as electrolyte. Cyclic voltammograms (CV) of MoO_2 electrodes were collected in the potential range of -1.2 to -0.5 V vs. SCE using ZAHNER-Elektrokemische Workstation IM6. Galvanostatic discharge and charge tests were performed with a cycle tester from LAND Electronic Co. The specific capacitance of MoO_2 electrode was calculated from CV curves (see Supporting information).

3. Results and discussion

TEM image (Fig. 1a) reveals that $m\text{-MoO}_2$ possesses an ordered mesoporous structure, which is an inverse replica of KIT-6 template. The thickness of the interconnected pore walls observed from SEM images (Fig. S1) is about 8 nm, close to the pore diameter of silica template (Fig. S2). Nitrogen sorption isotherm analyses on $m\text{-MoO}_2$ (Fig. 1b) indicate that it has a narrow pore size distribution centered at 13 nm and its specific surface area calculated by BET method is $69 \text{ m}^2 \text{ g}^{-1}$. XRD pattern (Fig. 1c) of $m\text{-MoO}_2$ can be indexed to distorted rutile MoO_2 phase (JCPDF No. 65-5787).

Elemental composition of $m\text{-MoO}_2$ was analyzed through EDX spectrum (Fig. 1d), which discloses the presence of Mo and O without any other impurities. The atomic ratio of Mo/O is determined to be 1/2, further validating the chemical composition of MoO_2 .

EQCM is a powerful tool that can monitor in-situ mass changes of electrode down to nanogram level during electrochemical process. By studying the relationship between the mass change and total charge passed through the electrode, the electrochemical mechanism can be analyzed. CV curve and the corresponding mass change of $m\text{-MoO}_2$ electrode during electrochemical cycles in 1 M LiOH solution are shown in Fig. 2a. During the reductive scan, the mass increases almost linearly, implying incorporation of cations into the $m\text{-MoO}_2$ electrode along with the electron gain. On the contrary, a mass loss is observed for the oxidative scan. Mass changes of $m\text{-MoO}_2$ electrode ($\Delta m \text{ (ng}^{-1}\text{)}$) are plotted against the stored charge (Q/C) during CV scan (Fig. 2b). The molecular weight (M) of working ions causing mass changes of MoO_2 electrode can be calculated according to the following equation:

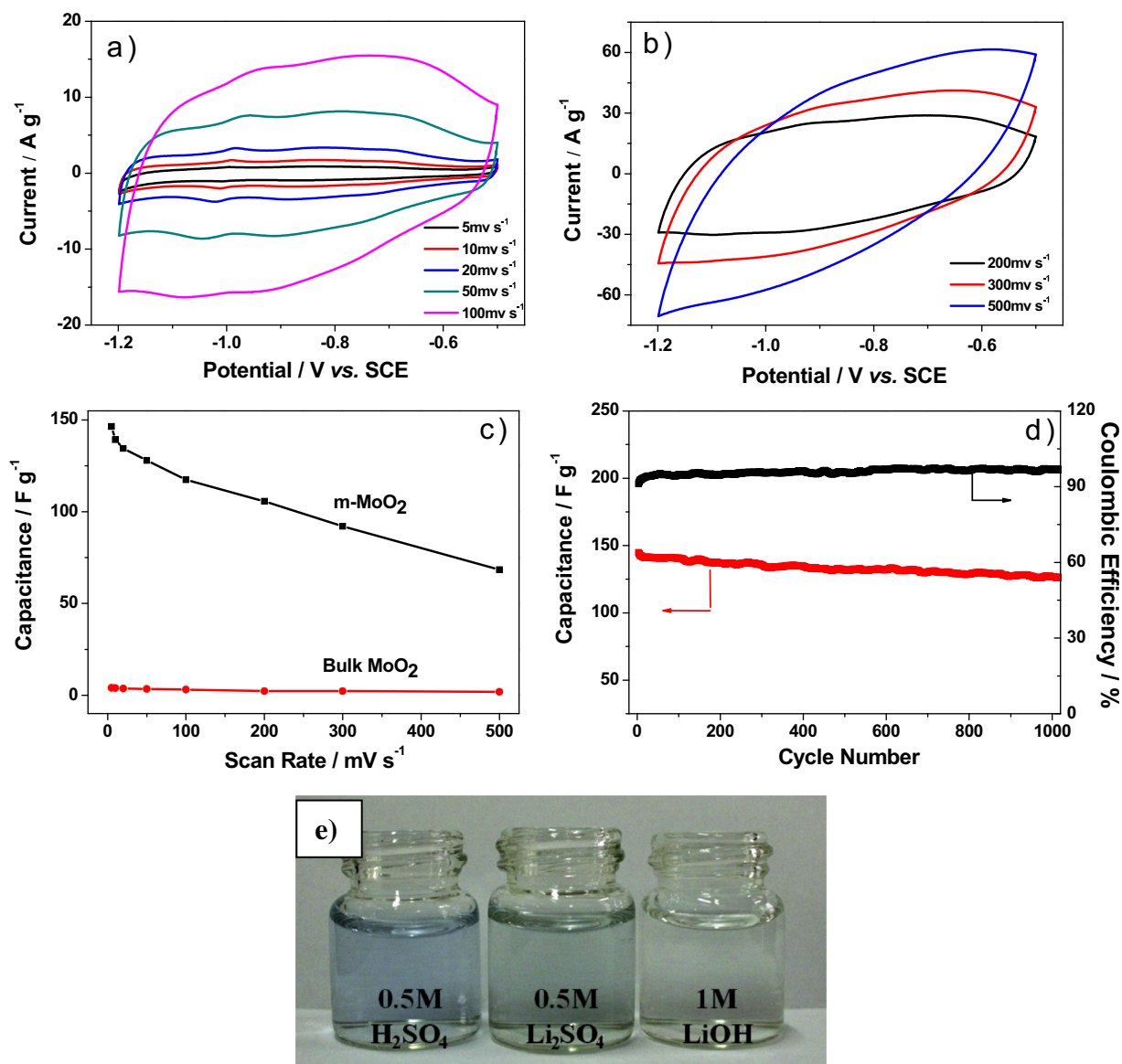


Fig. 3. a, b) CV curves of $m\text{-MoO}_2$ at various scan rates. c) Capacitance of $m\text{-MoO}_2$ and bulk MoO_2 at various scan rates. d) Cycling performance of $m\text{-MoO}_2$ discharged/charged at the current density of 1 A g^{-1} . e) Dissolution results of $m\text{-MoO}_2$ in three types of electrolyte.

$$M = 96,487 \times \Delta m \times 10^9 / \Delta Q \quad (1)$$

The calculated M from the slope of a–b and c–d parts denoted in Fig. 2b is 7 and 12 g mol^{−1}, respectively, resembling to the molecular weight of Li⁺. Thus Li⁺ ions can be regarded as the dominating working ions for the charge storage of m -MoO₂ in LiOH solution. As far as we know, the electrochemical mechanism of MoO₂ in aqueous electrolyte has never been reported by other researchers.

CV curve of m -MoO₂ (Fig. 2a) presents a rough rectangular shape, indicative of its supercapacitive nature. Besides the rectangular part, a couple of small redox peaks at about −0.92 V can be observed distinctly. It has been proposed that, the faradaic pseudocapacitance storage of transition-metal oxides mainly occurs in two manners, namely, adsorption of cations onto the surface of a material (adsorption pseudocapacitance) and intercalation of cations into the interlayer gaps of a material (intercalation pseudocapacitance) [22,23]. Both of them are accompanied by metal reduction. For the current m -MoO₂ material, the small couple of redox peaks in CV curve can be attributed to the intercalation/deintercalation of Li⁺ into/from the tunnel structure of MoO₂. The rectangular part arises from the adsorption/desorption of Li⁺ onto/from the m -MoO₂ surface. In comparison with LiOH electrolyte, CV curve of m -MoO₂ in Li₂SO₄ electrolyte presents a similar rectangular shape and a couple of distinct redox peaks (Fig. S5), also confirming that Li⁺ ions are the dominating working ions. The adsorption/intercalation behavior of Li⁺ onto/into m -MoO₂ is similar to that of MnO₂ material [24]. A schematic is presented in Fig. 2c to illustrate the adsorption and intercalation pseudocapacitance of m -MoO₂.

In order to test the electrochemical performance of m -MoO₂ for supercapacitors application, m -MoO₂ working electrode was prepared by pressing a mushy mixture of MoO₂, acetylene black, and poly(tetrafluoroethylene) onto Ni-mesh. Its CV curves in the potential range of −0.5 to −1.2 V vs. SCE at various scan rates are displayed in Fig. 3a and b. The redox peaks as well as the rectangular shape of m -MoO₂ are maintained rather well even at the scan rate of 100 mV s^{−1}, suggesting that both the adsorption and intercalation process of m -MoO₂ are kinetically facile. The specific capacitance (Fig. 3c) of m -MoO₂ at the scan rate of 5 mV s^{−1} is 146 F g^{−1}, close to that of MoO₂ nanorods (140 F g^{−1}) [25], well-aligned MoO₂ nanorods (205 F g^{−1}) [17], and carbon/MoO₂ nanocomposite (150 F g^{−1}) [26]. The capacitance is also considerably higher than those of MoO₃ nanorods (32 F g^{−1}) [27] and MoO₃ nanowires (96 F g^{−1}) [18]. Remarkably, the average working potential of m -MoO₂ is up to −0.85 V vs. SCE in LiOH electrolyte, making it suitable as an anode material for aqueous supercapacitors. When the scan rate increases to 500 mV s^{−1}, 47% of primary capacitance is preserved, signifying an excellent high rate capability of m -MoO₂. This can be ascribed to the highly ordered mesoporous structure and good electrical conductivity of m -MoO₂ [12], thus facilitating diffusion of electrolyte and transport of electrons. In contrast, bulk MoO₂ prepared free of silica template exhibits a very poor electrochemical activity.

The long-term cycling performance of m -MoO₂ electrode (Fig. 3d) is evaluated by galvanostatically discharging/charging it at the current density of 1 A g^{−1}. There is a slight capacitance loss of 10% after 1000 cycles. Actually, molybdenum oxides have not proven to be of much interest for aqueous supercapacitor applications because of their poor cycling behavior [28] associated with the high dissolution of Mo into electrolyte. Usually, H₂SO₄, Li₂SO₄, and Na₂SO₄ aqueous solutions were adopted as the electrolytes for molybdenum oxides [9,15–18,25–27], different from the electrolyte used in this work. Herein, a dissolution experiment of MoO₂ in three types of aqueous electrolytes with different pH was conducted. The same amounts of m -MoO₂ were added into 0.5 M

H₂SO₄, 0.5 M Li₂SO₄, and 1 M LiOH solution, respectively. After being stirred overnight at room temperature, these solutions were centrifuged to remove the m -MoO₂ precipitants. The colors of the final clear solutions (Fig. 3e) indicate that dissolution of m -MoO₂ in H₂SO₄ and Li₂SO₄ solutions is more serious than that in LiOH solution, which explains the good cycling performance of m -MoO₂ in LiOH solution.

4. Conclusion

Ordered mesoporous MoO₂ was prepared using silica KIT-6 as hard template. The dominating working ions for the charge storage of m -MoO₂ in aqueous LiOH electrolyte are proved to be Li⁺ ions through EQCM measurement. Owing to the ordered mesoporous structure and low solubility of MoO₂ in alkaline LiOH solution, m -MoO₂ exhibits an excellent high rate capability and good cycling performance. With an average working potential of −0.85 V vs. SCE, m -MoO₂ is suitable as an anode material for aqueous supercapacitors.

Acknowledgment

This work was supported by National Natural Science Foundation of China (NSFC No. 21203133, 21073129 and 51272168) and The Natural Science Foundation of Jiangsu Province (BK2012186).

Appendix A. Supplementary data

Supplementary data related to this article can be found at <http://dx.doi.org/10.1016/j.jpowsour.2013.03.020>.

References

- [1] P. Simon, Y. Gogotsi, Nat. Mater. 7 (2008) 845–854.
- [2] H. Zhu, X. Wang, X. Liu, X. Yang, Adv. Mater. 24 (2012) 6524–6529.
- [3] X. Wang, A. Sumboja, M. Lin, J. Yan, P.S. Lee, Nanoscale 4 (2012) 7266–7272.
- [4] G.Q. Zhang, H.B. Wu, H.E. Hoster, M.B. Chan-Park, X.W. Lou, Energy Environ. Sci. 5 (2012) 9453–9456.
- [5] J. Shao, X. Li, Q. Qu, H. Zheng, J. Power Sourc. 219 (2012) 253–257.
- [6] J. Shao, X. Li, Q. Qu, Y. Wu, J. Power Sourc. 223 (2013) 56–61.
- [7] J. Chang, J. Sun, C. Xu, H. Xu, L. Gao, Nanoscale 4 (2012) 6786–6791.
- [8] S. Chen, J. Zhu, X. Wang, ACS Nano 4 (2010) 6212–6218.
- [9] W. Tang, L. Liu, S. Tian, L. Li, Y. Yue, Y. Wu, K. Zhu, Chem. Commun. 47 (2011) 10058–10060.
- [10] Q. Qu, S. Yang, X. Feng, Adv. Mater. 23 (2011) 5574–5580.
- [11] Q. Qu, Y. Zhu, X. Gao, Y. Wu, Adv. Energy Mater. 2 (2012) 950–955.
- [12] Y. Shi, B. Guo, S.A. Corr, Q. Shi, Y.-S. Hu, K.R. Heier, L. Chen, R. Seshadri, G.D. Stucky, Nano Lett. 9 (2009) 4215–4220.
- [13] Y. Sun, X. Hu, J.C. Yu, Q. Li, W. Luo, L. Yuan, W. Zhang, Y. Huang, Energy Environ. Sci. 4 (2011) 2870–2877.
- [14] F. Gao, L. Zhang, S. Huang, Mater. Lett. 64 (2010) 537–540.
- [15] J. Jiang, J. Liu, S. Peng, D. Qian, D. Luo, Q. Wang, Z. Tian, Y. Liu, J. Mater. Chem. A 1 (2013) 2588–2594.
- [16] G.-R. Li, Z.-L. Wang, F.-L. Zheng, Y.-N. Ou, Y.-X. Tong, J. Mater. Chem. 21 (2011) 4217–4221.
- [17] L. Zheng, Y. Xu, D. Jin, Y. Xie, J. Mater. Chem. 20 (2010) 7135–7143.
- [18] R. Liang, H. Cao, D. Qian, Chem. Commun. 47 (2011) 10305–10307.
- [19] B. Hu, L. Mai, W. Chen, F. Yang, ACS Nano 3 (2009) 478–482.
- [20] D.O. Scanlon, G.W. Watson, D.J. Payne, G.R. Atkinson, R.G. Egdell, D.S.L. Law, J. Phys. Chem. C 114 (2010) 4636–4645.
- [21] T.-W. Kim, F. Kleitz, B. Paul, R. Ryoo, J. Am. Chem. Soc. 127 (2005) 7601–7610.
- [22] T. Brezesinski, J. Wang, S.H. Tolbert, B. Dunn, Nat. Mater. 9 (2010) 146–151.
- [23] T. Brezesinski, J. Wang, J. Polleux, B. Dunn, S.H. Tolbert, J. Am. Chem. Soc. 131 (2009) 1802–1809.
- [24] Q. Qu, P. Zhang, B. Wang, Y. Chen, S. Tian, Y. Wu, R. Holze, J. Phys. Chem. C 113 (2009) 14020–14027.
- [25] J. Rajeswari, P.S. Kishore, B. Viswanathan, T.K. Varadarajan, Electrochem. Commun. 11 (2009) 572–575.
- [26] Y. Zhou, C.W. Lee, S.K. Kim, S. Yoon, ECS Electrochem. Lett. 1 (2012) A17–A20.
- [27] I. Shakir, M. Shahid, H.W. Yang, D.J. Kang, Electrochim. Acta 56 (2010) 376–380.
- [28] W. Tang, L. Liu, Y. Zhu, H. Sun, Y. Wu, K. Zhu, Energy Environ. Sci. 5 (2012) 6909–6913.